16th World Conference on Earthquake, 16WCEE 2017
Santiago Chile, January 9th to 13th 2017
Paper N° 4006 (Abstract ID)
Registration Code: S-C1463148534

SEISMIC ISOLATION OF AN AMMONIA TANK IN TURKEY THROUGH PENDULUM ISOLATORS

M. G. Castellano[1], L. Marcolin[2]

[1] Senior Engineer, R & D Department, FIP Industriale S.p.A., maria.gabriella.castellano@fip-group.it
[2] Engineer, R & D Department, FIP Industriale S.p.A., luca.marcolin@fip-group.it

Abstract

The paper describes the seismic isolation system for an ammonia tank located in Samsun, Turkey, an area characterised by high seismicity; the PGA values for Design Basis Earthquake (DBE-475 years return period) and Maximum Credible Earthquake (MCE-2475 years return period) are 0.278 g and 0.490 g, respectively.

The supporting structure was already existing, thus one of the design criteria for the isolation system has been the reduction of base shear to a value lower than the elastic limit of the supporting structure. In effects, a response modification factor equal to one has been considered at all design level earthquakes, including MCE, due to the criticality of the structure.

The seismic isolation system includes three types of double concave curved surface sliders (or friction isolation pendulums with two primary concave sliding surfaces) characterized by equivalent radius of curvature of 4.5 m, seismic vertical load capacity ranging from 1840 to 3100 kN, and ± 450 mm displacement capacity. In total there are 121 isolators. The average dynamic friction coefficient guaranteed by such isolation system is 6.2 %.

The preliminary design of the isolation system has been carried out through nonlinear time history analyses on a simplified 3 masses model representing the impulsive and convective modes of vibration of the tank-liquid system, as well as the tank structure. Three couples of ground motion records have been used for such analyses, in particular Erzincan 1992, Kocaeli 1999 (Izmit station), amd Duzce 1999, properly scaled to respect the compatibility with the design spectrums (DBE and MCE). Peak values of the response parameters were used for design.

The maximum base shear obtained from the analyses is 8.4% of the seismic weight at DBE, while the maximum displacement is 359 mm at MCE.

Type Tests on two isolators per type have been carried out according to EN 15129, with some slight changes required by the Client. Additionally, two factory production control tests have been carried out, in order to check at least one isolator every 20 identical units. In total, 8 isolators have been tested.

Keywords: seismic isolation; tank; friction isolation pendulum

1. Introduction

Nowadays seismic isolation is frequently used worldwide for bridges and viaducts, for strategic buildings, e.g. hospitals, and in some countries for private buildings as well (residential and office buildings). The use of seismic isolation for industrial tanks is less frequent, but is rapidly increasing thanks to its benefits for such type of structures, demonstrated for example for LNG tanks and spherical tanks within the framework of the research project INDEPTH [1], [2], [3], [4]. In effects, seismic isolation can assure feasibility of tanks even in high seismicity areas.

This paper presents a recent example of application of seismic isolation in an ammonia tank located in an high seismicity area.

2. Description of the tank

The object of this work is the retrofit of a refrigerated storage tank, filled with liquefied ammonia, by means of seismic isolation with pendulum isolators with two primary concave sliding surfaces (called Double Concave Curved Surface Sliders according to the European Standards) manufactured by FIP Industriale.

The ammonia tank is a double wall refrigerated steel tank, with a capacity of about 22000 m^3. It bears on a concrete slab supported by 121 square columns, that are fixed to the foundation slab as represented in Fig. 1. The liquid storage tank is located in Tekkeköy, Samsun region of Turkey. Due to the high seismicity of the area, the requirements of the reference design code API 620 [1] cannot be fulfilled with the existing substructure (Fig. 1), in terms of reinforced concrete columns strength as well as sliding verification at the base of the tank. In order to avoid the re-configuration of the tank, the seismic isolation is the most effective solution. Thus, the fundamental design criteria for the isolation system has been the reduction of base shear to a certain value, lower than the elastic limit of the supporting structure and the sliding resistance. In effects, a response modification factor equal to one has been considered at all design level earthquakes, including MCE, due to the criticality of the structure.

In order to install the devices, the existing 121 columns were cut to create the proper room for the subsequent positioning of the isolator and the upper and lower steel anchor frames. After the completion of the installation of the devices, a new double wall refrigerated steel tank was placed over the existing isolated base.

The seismic isolation system is composed by three types of devices that differ by vertical load capacity and coefficient of friction. The equivalent radius of curvature and the displacement capacity are respectively 4.5 m and 450 mm, for all the devices types. Table 1 summarizes the numbers and the characteristics of the isolators designed for the ammonia tank. The isolators plan layout is shown in Fig. 2.

Fig. 1 – Picture from the site: existing concrete slab and foundation.

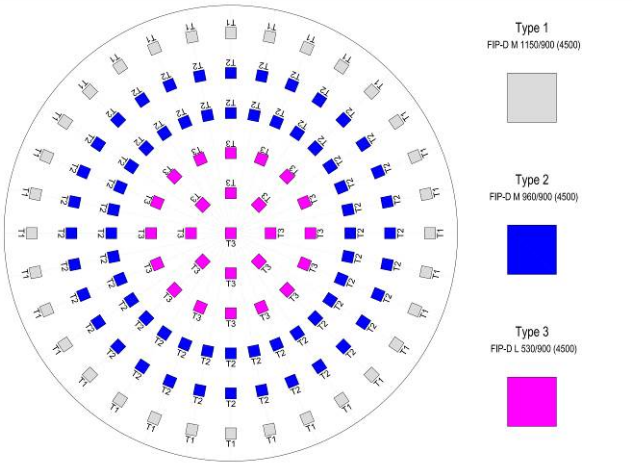

Fig. 2 – Seismic isolators layout plan.

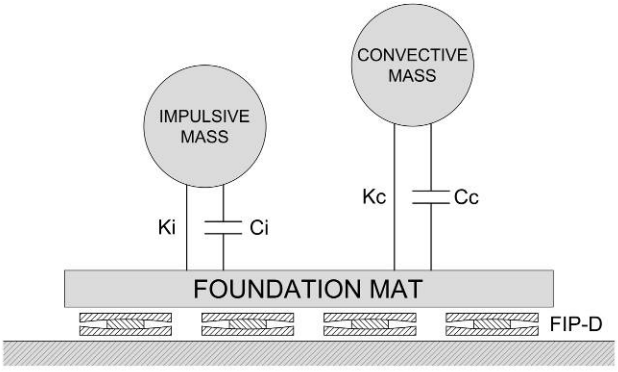

Fig. 3 – Schematization of the simplified model used in the analyses.

Table 1 - Quantity and main characteristics of double concave curved surface sliders used for the tank.

Isolator Type	Isolator mark	Max vertical load at ULS seismic N_{Ed} [kN]	Max vertical load at ULS static F_{zd} [kN]	Nominal coefficient of dynamic friction at N_{Ed}	Plan dimension of the device (Circum-square) [cm]	Nos.
1	***FIP-D M 1150/900 (4500)***	*3100*	*4000*	*5.5%*	*91 x 91*	*32*
2	***FIP-D M 960/900 (4500)***	*2110*	*3000*	*5.5%*	*87 x 87*	*64*
3	***FIP-D L 530/900 (4500)***	*1840*	*2750*	*2.5%*	*78 x 78*	*25*

Maximum vertical load at ULS load combinations including seismic actions (N_{Ed}):

$N_{Ed} \geq 1.0\ G + 1.0\ Q + 1.0\ |EQ_{MCE}|$

Maximum vertical load at ULS static load combination (F_{zd}):

$F_{zd} \geq 1.4\ G + 1.6\ Q$

Maximum displacement capacity (d_{Ed}): ±450 mm

Equivalent radius of curvature (R_{eq}): 4500 mm

Maximum rotation combined with maximum displacement (α): ±0.005 rad

3. Modelling

The dynamic behaviour of a liquid-storage steel tank, supported on a large concrete mat, may be adequately represented considering only the first impulsive and the first convective modes of vibration. Therefore a simplified model composed by two uncoupled single-degree-of-freedom (SDOF) systems may be used: one SDOF relevant to the impulsive part of the fluid and the other relevant to the convective part [6] [7]. In the case of a refrigerated and seismically isolated tank, the model becomes more complex, but the approach may be similar. Besides the above, the inertial contribution of the concrete mat and the external tank wall (outer shell) shall be considered.

The model used to evaluate the global dynamic behaviour of the seismically isolated ammonia tank is mainly composed by three uncoupled SDOF systems that bear upon a special finite element that represent the isolation system as a whole. In particular the three SDOF systems are associated to: 1) the impulsive component of the content fluid; 2) the convective component of the content fluid; and 3) the concrete mat (foundation) and the external tank wall (outer shell) both considered rigidly connected to the isolation system. The first and the second SDOF systems are defined as a mass, a spring and a dashpot, instead the third is defined as a mass only. The scheme of the model is illustrated in Fig. 3.

In order to define the parameters mentioned above, the natural period, the associated mass and the height of the latest in respect to the foundation of each SDOF system are calculated by the method described in API 650 [8] based on the theory of Housner [9]. The stiffness of the springs, associated to the impulsive (K_i) and convective (K_c) components, are calculated starting from the natural periods (T_i, T_c), and the masses (M_i, M_c). The dashpot damping capacity (C_i, C_c) is calculated assuming an effective damping ratio that considers the behaviour of the component, i.e. impulsive or convective, and the investigated seismic level effects, i.e. DBE or MCE. All the parameters defined above are summarized in Table 2.

The non linear behavior of the isolation system (as a whole) is considered in the model by means of a special finite element, a non-linear link, generally available in FE softwares. As described above, the isolation system of Samsun ammonia tank is composed by Double Concave Curved Surface Sliders (DCCSSs), characterized by an equivalent radius of curvature of 4.5 m and an average dynamic coefficient of friction equal to 6.2%.

Table 2 – Design parameters considered for the design of seismic isolation of the Samsun ammonia tank.

Number of isolators	121
Inner tank diameter (D)	29.988 m
Design liquid level (H)	31.061 m
Eq. uniform thickness of tank shell (t_u)	15.81 mm
Density of product stored (ρ)	683 kg/m^3
Weight of empty tank (W_0)	26300 kN
Total weight of the tank content (W_p)	165994 kN
Effective impulsive portion of the liquid weight ($W_i = M_i * g$)	131058 kN
Effective convective (sloshing) portion of the liquid weight ($W_c = M_c * g$)	36823 kN
Natural period of vibration for impulsive mode (T_i)	0.34 s
Natural period of vibration for convective (sloshing) mode (T_c)	5.70 s
Effective stiffness associated to the impulsive portion of the liquid weight (K_i)	4538935 kN/m
Effective stiffness associated to the convective portion of the liquid weight (K_c)	4563 kN/m
Effective damping ratio for impulsive mass (DBE – MCE)	2.0% - 4.0%
Effective damping ratio for convective mass	0.5%

4. Seismic input

The ammonia tank described in this paper is located in Tekkeköy, in the Samsun region, Turkey. In order to define the seismicity of the area, a site specific seismic hazard analysis was carried out by the Engineer of the Civil Structures. In accordance with the Turkish Code TEC 2007 [11], the site is located in seismic zone 2 and the soil investigation report indicates the site soil as Z3. Soil groups and local site classes to be considered as the bases of determination of local soil conditions are given in Table 3 and Table 4 respectively. Values concerning soil parameters in Table 3 are to be considered as standard values given - by the code - for guidance in determining the soil groups.

The spectra have been defined for different serviceability level earthquakes, in particular, for earthquakes with return periods of 75 years (Operating Basis Earthquake), 475 years (Design Basis Earthquake) and 2475 years (Maximum Credible Earthquake).

Starting from the above mentioned response spectra, three sets of Ground Motion Records (GMRs) have been selected and scaled to be used as input for the time history analyses. In particular, the GMRs of the earthquakes of Erzincan 1992 (RSN 821), Kocaeli 1999 (RSN 1165) and Duzce 1999 (RSN 1605) were selected from the NGA-West2 ground motion database [12]. The indicated Record Sequence Number (RSN) for each GMR refers to said database. The mentioned earthquakes are characterized by a magnitude in the range 6.7 ÷7.5,

a fault distance less than 10 km (near fault) and by a source mechanism type Strike Slip (SS). Fig. 4 shows the SRSS of the response spectra of the two horizontal component of each scaled Ground Motion Record, in comparison with the site specific response spectra for the DBE and MCE seismic levels.

Table 3 – Soil Groups [11]

Soil Group	***Description of Soil Group***	***Standard Penetration (N/30)***	***Relative Density (%)***	***Unconfined Compressive Strength (kPa)***	***Drift Wave Velocity (m / s)***
(A)	1. Massive volcanic rocks, unweathered sound metamorphic rocks, stiff cemented sedimentary rocks 2. Very dense sand, gravel... 3. Hard clay and silty clay…	---- > 50 > 32	---- 85 -- 100 ----	> 1000 ---- > 400	> 1000 > 700 > 700
(B)	1. Soft volcanic rocks such as tuff and agglomerate, weathered cemented sedimentary rocks with planes of discontinuity…… 2. Dense sand, gravel..... 3. Very stiff clay, silty clay…	---- 30 50 16 32	----- 65 -- 85 ----	500 -- 1000 ---- 200 -- 400	700 -- 1000 400 -- 700 300 -- 700
(C)	1. Highly weathered soft metamorphic rocks and cemented sedimentary rocks with planes of discontinuity 2. Medium dense sand and gravel.....……. 3. Stiff clay and silty clay.....	---- 10 -- 30 8 -- 16	---- 35 -- 65 ----	< 500 ---- 100 -- 200	400 -- 700 200 -- 400 200 -- 300
(D)	1. Soft, deep alluvial layers with high ground water level 2. Loose sand.....….. 3. Soft clay and silty clay…..	---- < 10 < 8	---- < 35 ----	---- ---- < 100	< 200 < 200 < 200

Table 4 – Local Site Classes [11]

Local Site Class	***Soil Group according to Table 6.1 and Topmost Soil Layer Thickness*** **(h_1)**
Z1	Group **(A)** soils Group **(B)** soils with $h_1 \leq 15$ m
Z2	Group **(B)** soils with $h_1 > 15$ m Group **(C)** soils with $h_1 \leq 15$ m
Z3	Group **(C)** soils with 15 m < $h_1 \leq 50$ m Group **(D)** soils with $h_1 \leq 10$ m
Z4	Group **(C)** soils with $h_1 > 50$ m Group **(D)** soils with $h_1 > 10$ m

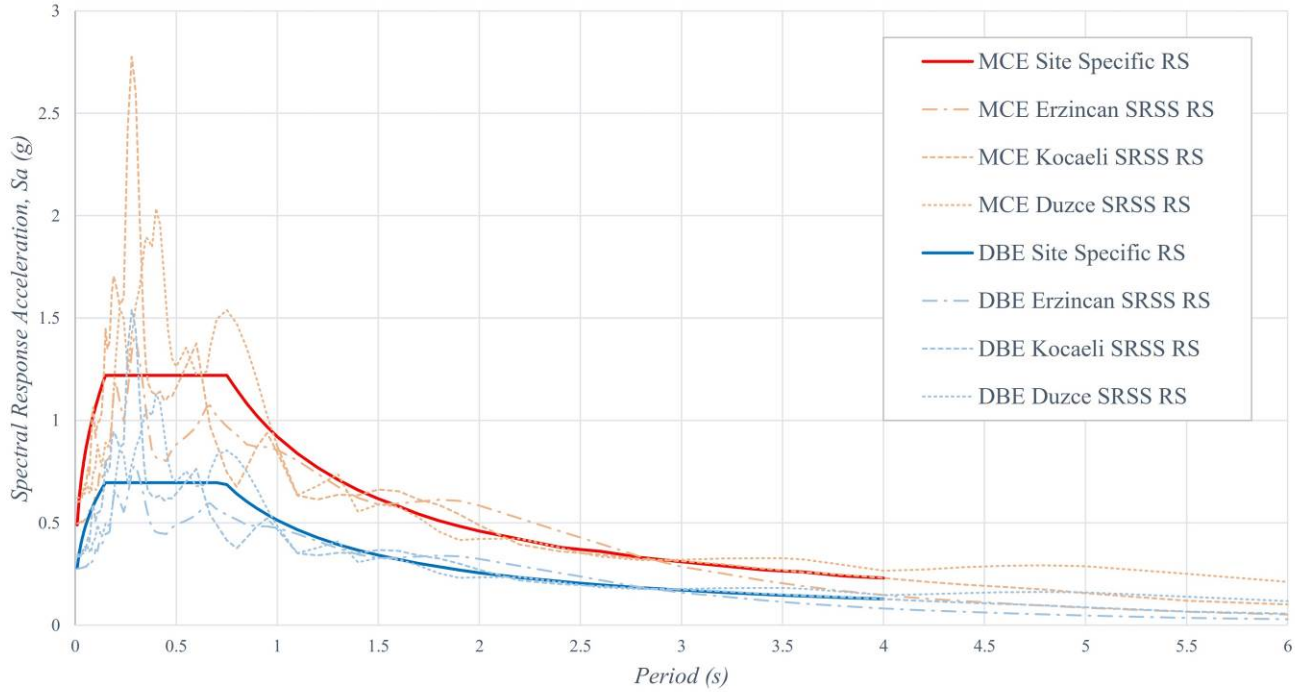

Fig. 4 – Comparison between the Site Specific Response Spectra (RS) and the SRSS Response Spectra of the selected and scaled Ground Motion Records.

5. Results

The dynamic behavior of the Samsun Ammonia tank was evaluated performing non-linear time history analysis on the simplified model described above, with different properties of the seismic isolation system, in order to select the isolation system that guarantees the best results. Here only the results obtained with the finally selected isolation system are presented.

The three sets of scaled Ground Motion Records were used as time history data input for both the MCE and DBE seismic levels. In the analyses the possible variations of the characteristics of the isolation system property were considered (upper and lower bound analyses). In particular, the value of the nominal friction coefficient of the devices, and of the isolation system as a whole as a consequence, was varied by means of proper modification factors.

The maximum displacement and the maximum base shear of the isolation system have been calculated from the vectorial sum of the two orthogonal components at each time step, for each Ground Motion record used for the response-history analysis. Since the number of analyzed GMRs is lower than seven, the maximum values of the response parameters have been used for design [13].

The results of the non-linear time history analyses on the simplified tank model, are shown below only for the full tank condition at nominal values of the isolation system properties. The results of the empty tank (or with different levels of filling) condition analyses are no relevant for the design of the isolation system.

The results of the non-linear time history analyses, in terms of total base shear and displacement of the isolation system, are respectively represented in Fig. 5 left and right, considering the nominal characteristics of the devices, for the Design Basis Earthquake (DBE) and Maximum Credible Earthquake (MCE). It is worth noting that the upper limit base shear vs. total weight ratio for this project was 11% for DBE level, and the maximum allowable displacement was 450 mm for the MCE level.

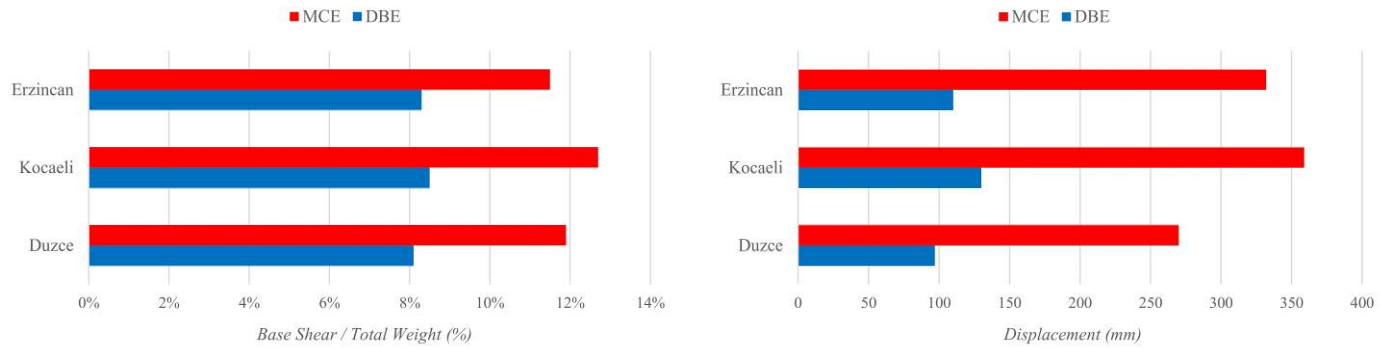

Fig. 5 - Results of the non linear time history analyses,
in terms of base shear vs. total weight ratio (left) and displacement (right), for DBE and MCE.

From Fig. 5 it is evident that the most severe seismic input is the Kocaeli 1999 (RSN 1165) ground motion record; the maximum response parameters are within the upper limiting values, in particular the maximum base shear vs. total weight ratio is equal to 8.4% for DBE level (less than the limiting 11%), and the maximum displacement is 359 mm for the MCE level (less than the limiting 450 mm).

Further results with this input are reported in Fig. 6 and Fig. 7, respectively for DBE and MCE levels. The graphs show the comparison between the seismic input and the response in terms of accelerations, separately for the two main orthogonal horizontal directions and for the two earthquake levels. The time histories of the acceleration for the impulsive and convective masses are reported separately, in order to focus on the two main characteristics of the seismically isolated storage tanks: the acceleration of the impulsive part of the fluid is strongly mitigated by the isolation system, while the response modification for the convective part of the fluid is negligible. The reason of this behavior is related to the fact that the impulsive period (T_i), even though shifted by the isolation system, is still significantly lower than the convective period (T_c).

The beneficial effect achieved with the implementation of the isolation system can be estimated in terms of the ratio between the peak ground acceleration (PGA) and the impulsive peak response acceleration of the system. Starting from the results reported in Fig. 7 (right) the PGA is equal to 4.78 m/s^2, while the maximum impulsive peak acceleration is equal to 1.57 m/s^2. In this case the implementation of the isolation system results in a reduction of the horizontal acceleration of 3 times compared to the PGA. If similar comparison is made with the impulsive peak acceleration of the non-isolated (fixed base) tank, the latter would be higher than PGA, because the period of the impulsive mode would correspond to the maximum amplification in the response spectrum.

The largest effective period associated to the isolation system, calculated at the maximum peak displacement obtained from the analyses, is equal to 2.4 s for the DBE level and equal to 3.2 s for the MCE level. Comparing the calculated peak effective periods with the period associated to the convective mass (T_c), the ratio between T_c (equal to 5.7 s) and the effective period of the isolation system results equal or greater than 2.4 for the DBE level and equal or greater than 1.8 for the MCE level.

Fig. 8 shows the force vs. displacement curve (left) and the horizontal displacement path curve (right) for the Duzce 1999 (RSN 1605) scaled at Maximum Credible Earthquake (MCE).

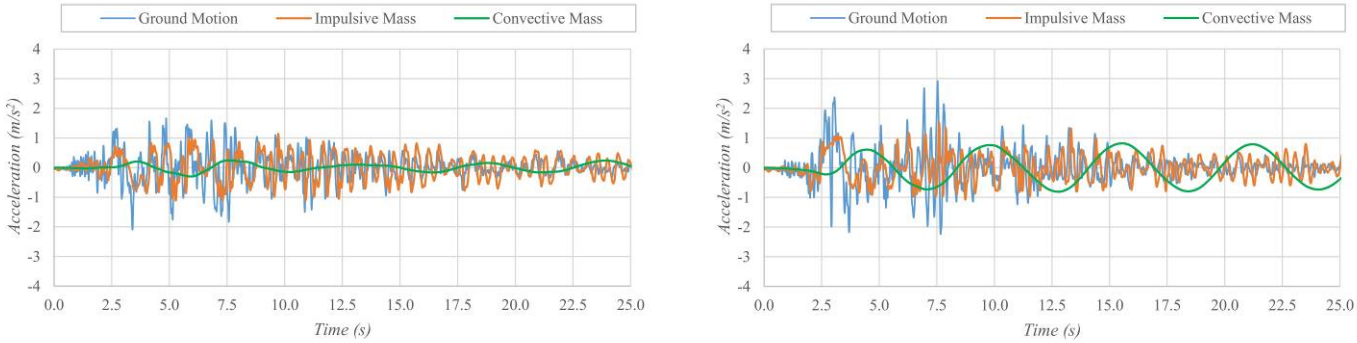

Fig. 6 – Comparison between the ground acceleration and the response of the impulsive and convective masses in terms of accelerations, for both the horizontal directions considering the Kocaeli 1999 earthquake scaled at the Design Basis Earthquake (DBE).

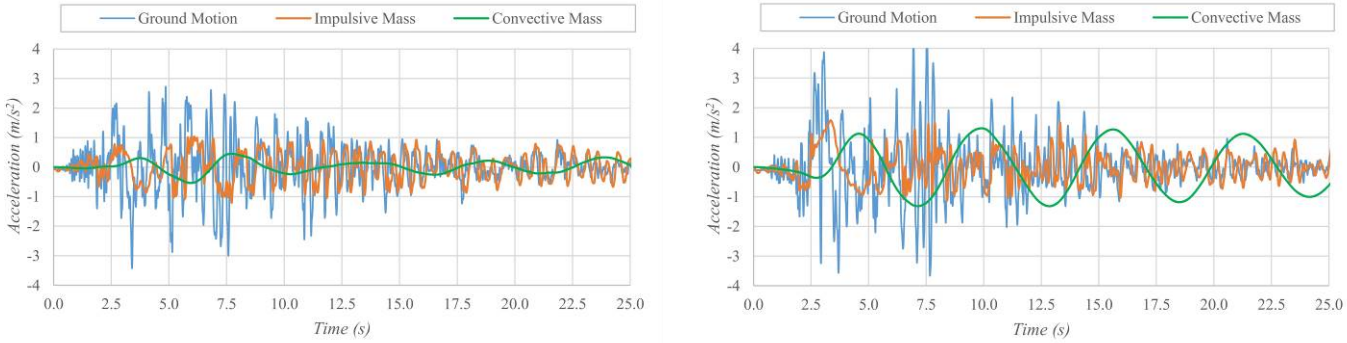

Fig. 7 – Comparison between the ground acceleration and the response of the impulsive and convective masses in terms of accelerations, for both the horizontal directions considering the Kocaeli 1999 earthquake scaled at the Maximum Credible Earthquake (MCE).

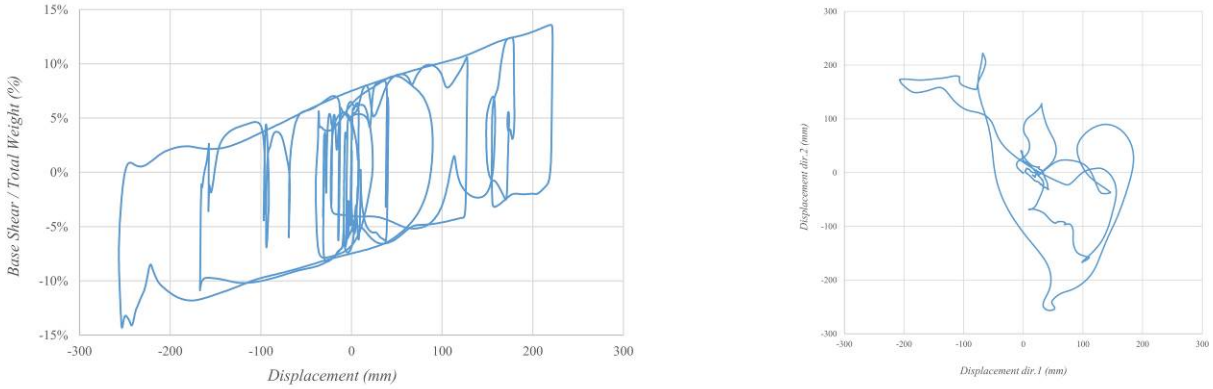

Fig. 8 - Force vs. displacement curve and displacement path curve for the Duzce 1999 (RSN 1605) scaled at Maximum Credible Earthquake (MCE).

6. Experimental tests

The Type Tests carried out at the FIP Industriale Laboratories, in Italy, were performed according to the European Standard on Anti-seismic devices EN 15129:2009 [14], carrying out a series of quasi-static and dynamic tests. Additionally to the test program required by the standard, due to the criticality of the structure, the client requested a supplementary dynamic sliding isolation test in which the applied horizontal displacement equals the maximum displacement capacity of the device (d_{Ed}) equal to 450 mm. The associated peak velocity (v_{Ed}) reached during the additional test was equal to 644 mm/s.

In this paper, for the sake of brevity, the procedure and the results of the additional dynamic sliding isolation test are presented. In effects said test is the most severe test in terms of energy dissipation demand for the device.

6.1 Test equipment

All tests were performed using the Biaxial Dynamic Test System – nominated as M1 – that enables the application of vertical loads in combination with horizontal movements at high velocities. It is characterized by 30000 kN vertical load capacity, 3000 kN transversal load, ±500 mm maximum total stroke and 1570 mm/s velocity (see Table 5, Fig. 9) [15].

Table 5 - Performance characteristics of the Biaxial Dynamic Test rig.

Characteristics	Value
Vertical Actuators F_{max} [kN] - Dynamic	20000
Vertical Actuators F_{max} [kN] - Static	30000
Horizontal Actuator F_{max} [kN]	3000
Total Horizontal Stroke [mm]	±500
Maximum Velocity [mm/s]	1570
Test sample room available [mm]	2000 x 2000 x 700

The tests were carried out on single isolator. The unit specimen under testing is installed between the top loading platen and the bottom moving platen.

The steel vertical test frame is designed to resist the vertical load applied to the unit specimen under testing coupled to a horizontal frame able to withstand the lateral load imposed to the unit. Four hydraulic vertical actuators are installed between the steel cross-beam and the loading platen. The specimen is installed between the loading platen and the bottom moving platen. The relative horizontal displacement is imposed to the specimen by moving the bottom platen connected to the horizontal actuator. In this way, the upper portion of the isolator can move according to the vertical load axis only whilst the lower portion is subjected to the main horizontal movement.

The measurements of the displacements and the horizontal loads have been carried out, using a displacement transducer SSI 1000 mm with 0.002 resolution and a Sensy load cell of 3000 kN, respectively; the vertical load was measured by means of HBM P3MB pressure transducers. The transducers were connected to the amplifier control system actuator (MTS Flex Test 60) whose output signals are acquired through a measuring amplifier Spider 8. This amplifier, connected via PC with data acquisition and processing software DIA Dem (National Instruments), provided the final signal then processed in the graphs.

The inertial effects were evaluated considering the average acceleration measured by means of two accelerometers type HBM B12-200 arranged according to the horizontal movement axes, and then extracted from the signal measured with the Sensy load cell arranged to the same axis.

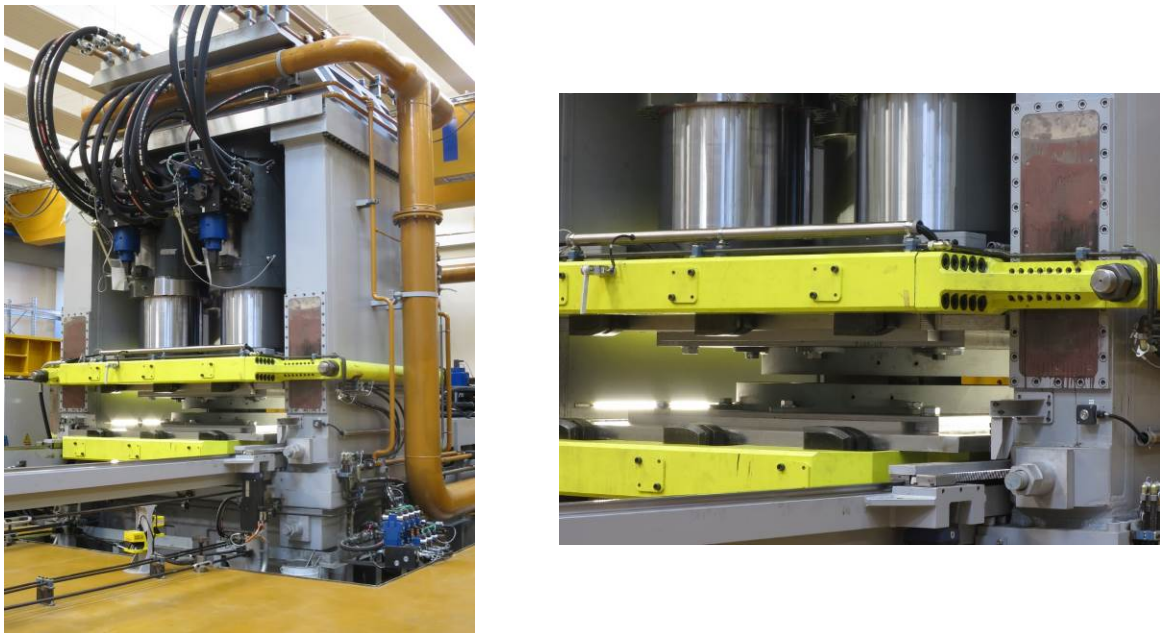

Fig. 9 - Biaxial test system - FIP Industriale Dynamic Test Laboratory.

6.2 Testing procedure

The testing procedure for the additional dynamic sliding isolation test is described here below.

At zero displacement, a vertical load equal to the non-seismic design load (N_{Sd}) was applied and kept constant. Three series of 3 fully reversed cycles, were imposed with an amplitude equal to the maximum capacity of the device (d_{Ed}). The displacement input waveform was sinusoidal.

The non-seismic vertical load (N_{Sd}), for each isolator type, is corresponding to the average value of the Quasi-Permanent load acting on all the isolators of the same type. The Quasi-Permanent load, in the case of a liquid storage tank, is the vertical load applied on the devices associated to the full tank loading condition. It is different for each device type, because of their plan distribution (Fig. 2).

The main frequency f_0 has been calculated as the reverse of the period associated to the restoring stiffness equal to Eq. 1, in which R is the equivalent radius of curvature and g is the gravity acceleration.

$$T = 2\,\pi\,(R / g)^{0.5} = 4.26 \text{ s} \tag{1}$$

So, the peak velocity shall be considered as Eq. 2: $v_{Ed} = \sqrt{\frac{g}{R}} \cdot d_{bd}$

$$v_{Ed} = (g / R)^{0.5}\, d_{Ed} = 664 \text{ mm/s} \tag{2}$$

6.3 Test results

The sliding isolation tests were performed in 3 fully reversed cycles, thus the dynamic coefficient of friction μ_{dyn} was calculated as Eq. 3:

$$\mu_{dyn} = \frac{1}{3}\sum_{i=1}^{3} \frac{A_{h,i}}{4 N_{Sd} d_{Ed}} \tag{3}$$

Fig. 10 and Table 6 present respectively the force-displacement curves and the results data obtained from the tested devices at maximum displacement capacity (d_{Ed}) and applying the non-seismic vertical load (N_{Sd}). In Fig. 10 (left and right) the two parallel blue lines drawn in the graph are useful to evaluate the restoring stiffness.

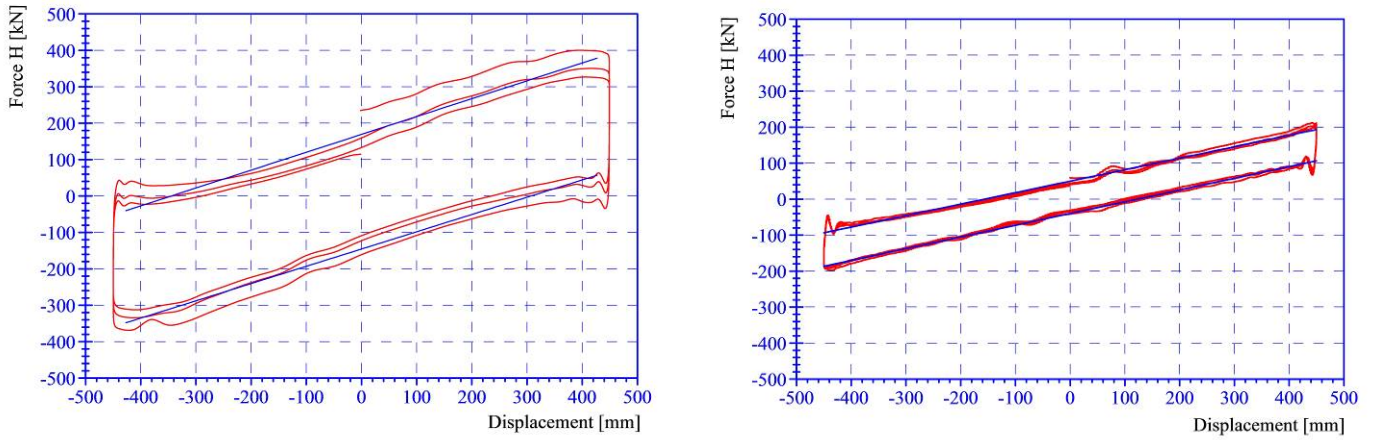

Fig. 10 - Hysteretic cycles obtained during the Dynamic Tests on
Isolator FIP-D M 1150/900(4500) (left) and isolator FIP-D L 530/900(4500) (right).

Table 6 – Test results of the additional dynamic sliding isolation test

Isolator Type	**Vertical Load N_{Sd} [kN]**	**Friction $\mu_{dyn,1}$ [%]**	**Average Friction $\mu_{dyn,3}$ [%]**	**Rest. Stiffness K_2 [kN/mm]**	**Average EDC [kJ]**
FIP-D M 1150/900(4500)	2210	8.67	7.02	0.481	279.2
FIP-D L 530/900(4500)	1503	3.64	3.09	0.322	83.9

The results of the Type Tests and the additional tests demonstrated that the double concave curved surface sliders behaves exactly as expected and they are in compliance with the European Standards. It was verified the reliability of the devices under static, service and dynamic performance. Under service conditions the devices exhibit a steady maximum reaction force in both directions also when subjected to a high numbers of cycles. A series of dynamic isolation tests at different amplitude and vertical load were performed, demonstrating a constant and stable force at all cycles in each test and constant energy dissipation.

7. Conclusions

The scope of this work was to investigate the dynamic behavior of a seismically isolated liquid storage tank by means of a 3DoF simplified model, in order to optimize the response of the isolation system.

The seismic isolation system of an ammonia tank located in Samsun, Turkey, an area characterised by high seismicity (PGA at MCE level equal to 0.490 g), has allowed to reuse the existing supporting structure.

The seismic isolation system includes three types of double concave curved surface sliders (or pendulum isolators with two primary concave sliding surfaces) characterised by equivalent radius of curvature of 4.5 m, seismic vertical load capacity ranging from 1840 to 3100 kN, and ± 450 mm displacement capacity. In total there are 121 isolators.

The results of the nonlinear time history analyses carried out on the simplified model show the effectiveness of seismic isolation in the reduction of the acceleration transmitted to the superstructure, for example with the most severe seismic input used (Kocaeli 1999) at MCE level the acceleration on the impulsive mass is less than 1/3 of the PGA.

Further analyses on more complex model have been carried out by the Structural Engineer, in order to validate the preliminary design - based on the simplified model of the liquid storage tank – and design the structure.

The results of the dynamic tests performed on the isolators confirm that their behaviour corresponds to the theoretical one.

8. Acknowledgements

The author thank the Engineer of the Civil Structures PROTA Engineering as well as to the Contractor CENGIZ, for the fruitful cooperation in this application.

9. References

[1] Crespo M., Omnes S., Marti J. (2006): Benefits of seismic isolation for LNG tanks. *Proceedings of 1st European Conference on Earthquake Engineering and Seismology*, Geneva, Switzerland, 3-8 September 2006, Paper No. 1083.

[2] Bergamo G., Castellano M.G., Gatti F., Rebecchi V. (2006): Parametric analyses for the seismic isolation of LNG tanks. *Proceedings of 1st European Conference on Earthquake Engineering and Seismology*, Geneva, Switzerland, 3-8 September 2006, Paper No. 1046.

[3] Gregoriou V.P., Tsinopoulos S.V., Karabalis D.L. (2006): Base isolated LNG tanks: seismic analyses and comparison studies. *Proceedings of 1st European Conference on Earthquake Engineering and Seismology*, Geneva, Switzerland, 3-8 September 2006, Paper No. 1128.

[4] Bergamo G., Castellano M.G., Gatti F., Poggianti A., Summers P. (2006): Seismic isolation of spheres at petrochemical facilities. *Proceedings of 1st European Conference on Earthquake Engineering and Seismology*, Geneva, Switzerland, 3-8 September 2006, Paper No. 1009.

[5] API Standard 620 (2013): Design and Construction of Large, Welded, Low-Pressure Storage Tanks, Annex L: Seismic Design of API 620 Storage Tanks. American Petroleum Institute.

[6] Malhotra PK (1997): New Method for Seismic Isolation of Liquid-Storage Tanks, *Earthquake Engineering and Structural Dynamics*, Vol. 26, 839-847.

[7] Malhotra PK, Wenk T, Wieland M (2000): Simple Procedure for Seismic Analysis of Liquid-Storage Tanks, *Structural Engineering International*, IABSE, Vol. 10, No.3, 197-201.

[8] API Standard 650 (2013): Welded Steel Tanks for Oil Storage, Annex E: Seismic Design of Storage Tanks. American Petroleum Institute.

[9] Housner GW (1963): Dynamic analysis of fluids in containers subjected to acceleration, *Nuclear Reactors and Earthquakes Report No. TID 7024*, U. S. Atomic energy Commission, Washington D.C.

[10] Haroun MA, Housner GW (1981): Seismic design of liquid storage tanks, *Journal of Technical Councils of ASCE*, Vol. 107, No. TC1, 191-207.

[11] Turkish Earthquake Design Code TEC 2007 (2009). Turkish Republic the Ministry of Public Works and Settlement, Ankara.

[12] NGA-West2 ground motion database: Pacific Earthquake Engineering Research Center (PEER).

[13] ASCE Standard ASCE/SEI 7-10 (2010): Minimum Design Loads for Building and Other Structures. American Society of Civil Engineers.

[14] UNI EN 15129 (2009): Anti-Seismic Devices, Comité Européen de Normalisation (CEN), Brussels.

[15] Infanti S, De Toni S, Pigouni AE (2015): Dynamic Testing Protocols for Seismic Protection Devices: New Challenges for Test Facilities, *Proceedings of 14th World Conference on Seismic Isolation, Energy Dissipation and Active Vibration Control of Structures*, San Diego, Ca USA.